Maximizing hydrogen production in a microbial electrolysis cell by real-time optimization of applied voltage

Tartakovsky, B.; Mehta, P.; Santoyo, G.; Guiot, S. R.

Publisher's version / Version de l'éditeur:
https://doi.org/10.1016/j.ijhydene.2011.05.162
International Journal of Hydrogen Energy, 36, 17, pp. 10557-10564, 2011-06-29

Available at www.sciencedirect.com

ScienceDirect

journal homepage: www.elsevier.com/locate/he

Maximizing hydrogen production in a microbial electrolysis cell by real-time optimization of applied voltage

B. Tartakovsky, P. Mehta, G. Santoyo, S.R. Guiot*

Biotechnology Research Institute, National Research Council of Canada, 6100 Royalmount Ave., Montréal, QC, Canada H4P 2R2

ARTICLE INFO

Article history:
Received 15 December 2010
Received in revised form
11 May 2011
Accepted 24 May 2011
Available online 29 June 2011

Keywords:
Microbial electrolysis cell
Real-time control
Optimization
perturbation/observation

ABSTRACT

This study describes a novel method for controlling applied voltage in a microbial electrolysis cell (MEC). It is demonstrated that the rate of hydrogen production could be maximized without excessive energy consumption by minimizing the apparent resistance of the MEC. A perturbation and observation algorithm is used to track the minimal apparent resistance by adjusting the applied voltage. The algorithm was tested in laboratory-scale MECs fed with acetate or synthetic wastewater. In all tests, changes in MEC performance caused by the variations in organic load, carbon source properties, and hydraulic retention time were successfully followed by the minimal resistance tracking algorithm resulting in maximum hydrogen production, while avoiding excessive power consumption. The proposed method of real-time applied voltage optimization might be instrumental in developing industrial scale MEC-based technologies for treating wastewaters with varying composition.

1. Introduction

Hydrogen production in microbial electrolysis cells (MECs) represent a novel bioelectrochemical process in which an energy carrier (hydrogen) is produced from renewable sources of organic matter such as organic wastes and residual biomass. H_2 production is accomplished by a combination of microbial processes at the anode, where exoelectrogenic microorganisms oxidize organic matter and electrochemical or bioelectrochemical processes at the cathode, where the electrons and protons are combined to form H_2 [1]. Although an external power source is required, the microbially catalyzed electrolysis of organic matter consumes significantly less energy than H_2 production via water electrolysis [2,3]. Furthermore, because of the broad selectivity of mixed microbial consortia, MECs can operate on a wide variety of organic materials, including wastewater [4,5]. Combining wastewater treatment with energy production is similar to the conventional anaerobic digestion process where methane is produced, but the MEC-based process produces a more valuable energy carrier, H2.

Recent advances in MEC research resolved several limitations, which were considered crucial for the development of an industrial MEC-based process. In particular, volumetric rates of H_2 production have surpassed 5–10 L L_R^{-1} d^{-1}, continuous operation of MECs have been demonstrated, and expensive Pt-based cathode – PEM designs were replaced with membraneless MECs equipped with non-noble Me catalysts such as Ni, stainless steel, or tungsten carbide [1,6–10]. These improvements make MEC scale-up more realistic, thus necessitating the development of a real-time process control system similar to maximum power point tracking (MPPT) systems developed for fuel cells [11]. The MPPT system could be used to adjust the energy input in accordance with variations in wastewater composition, concentration, conductivity, and other factors. In this study we demonstrate that a real-time control system can efficiently track the changes in the

* *Corresponding author*. Tel.: +1 514 496 2664; fax: +1 514 496 6265.
E-mail address: Boris.Tartakovsky@nrc-cnrc.gc.ca (B. Tartakovsky).

0360-3199/$ – see front matter Crown Copyright © 2011, Hydrogen Energy Publications, LLC. Published by Elsevier Ltd. All rights reserved.
doi:10.1016/j.ijhydene.2011.05.162

operating conditions of a MEC, while maintaining H_2 production at the maximum attainable level.

2. Materials and methods

2.1. Media solutions

The acetate stock solution contained (in g L^{-1}): sodium acetate (55.34), yeast extract (0.830), NH_4Cl (18.7), KCl (148.1), K_2HPO_4 (64.0), and KH_2PO_4 (40.7), corresponding to an acetate concentration of 40 g/L. A stock solution of synthetic wastewater (sWW) contained (in g L^{-1}) : pepticase (50), beef extract (50), yeast extract (30), NH_4HCO_3 (17), K_2HPO_4 (1.5), KH_2PO_4 (1.75). The sWW stock solution was prepared and frozen until used.

2.2. MEC operation and characterization

Two membraneless MECs were constructed with a series of nylon plates. Each MEC had a 50 mL anodic compartment and a H_2 collection compartment of the same volume (100 mL total setup volume). The anodic chamber contained a 5-mm thick GFA-5 carbon felt anode measuring 10 × 5 cm (SGL Group, Wiesbaden, Germany). The carbon paper gas diffusion cathode (GDL 25BC, SGL Group, Wiesbaden, Germany) contained 0.2 mg/cm^2 of electrodeposited Ni. The Ni deposition procedure is described in Manuel et al. [12]. The cathode was sandwiched between the anodic and the H_2 collection compartment plates forming a wall between the two compartments. A polyester cloth, approximately 0.7 mm thick, was placed between the two electrodes. More details on MEC design can be found elsewhere [7,13].

The MECs were inoculated with 5 mL of a homogenized anaerobic mesophilic sludge obtained from a local food processing industry (A. Lassonde Inc., Rougemont, Quebec, Canada) and were maintained at 30 °C and a pH of 6.8–7.0 using temperature and pH controllers, respectively. The acetate and sWW stock solutions were continuously fed at a rate of 5 mL d^{-1} using infusion pumps (model PHD 2000, Harvard Apparatus, Canada) with 60 mL syringes. The sWW stock solution was replaced every 2–4 days. Dilution water was continuously fed to MECs using peristaltic pumps connected to a timer. One mL of a trace metals solution [13] was added per liter of dilution water. The nutrients and dilution water streams were combined before entering the anodic compartment.

The acetate-fed (MEC-A) and sWW-fed (MEC-W) MECs were started up at a hydraulic retention time (HRT) of 9.8 h and 18.3 h, respectively. Throughout the tests HRTs and organic loads of the MECs were changed as outlined in Table 1. Four tests were carried out in each MEC. The tests (phases) performed during MEC-A operation included standard conditions, an increase in the organic loading rate (influent acetate concentration), an increased HRT, and a decrease in conductivity. The tests done for MEC-W operation included standard conditions, increased organic loading rate (influent concentration), a decrease in HRT, and a decrease in conductivity combined with a decreased HRT.The details are provided in Table 1. In between the experimental phases, the MECs were returned to the standard conditions before proceeding to the next test phase. The MECs were maintained in each test phase for 5–9 days to reach a new steady state.Overall, MEC-A and MEC-W were operated for 42 and 55 days, respectively.

The applied voltage was controlled using a computer-interfaced power source (PW18–1.8, Kenwood, Japan). The voltage applied, current, and gas flow were recorded using an on-line data acquisition system. Gas production in the MECs was measured by bubble counters (Innoray, Montreal, QC, Canada). Gas composition was measured using a 6890 Series gas chromatograph (Hewlett Packard, Wilmington, DE, USA). VFA analysis was performed by an Agilent 6890 gas chromatograph (Wilmington, DE, USA). The conductivity was measured using a conductivity meter (Accumet XL 30, Fisher Scientific, Pittsburgh, PA, USA). More details regarding MEC monitoring can be found elsewhere [13].

Voltage scans were performed at the end of each phase. The scans were performed by changing the applied voltage between +0.4 and +1.2 V, with 10-min intervals after each voltage change to allow the outputs to stabilize. The results were used to estimate optimal applied voltage, which corresponded to the minimal apparent resistance.

The MEC performance was characterized in terms of the volumetric H_2 production rate, expressed per liter of the reactor volume (L_R). Coulombic efficiency was calculated as the ratio of electrons relative to the total electrons available from acetate consumption. Cathodic efficiency was calculated as the ratio of electrons recovered as hydrogen gas to the total number of electrons that reach the cathode; and power consumption per liter of H_2 recovered in the off-gas. A detailed explanation can be found elsewhere [9,14].

2.3. Real-time control of applied voltage

The applied voltage (U_{app}) was periodically adjusted in order to minimize the apparent resistance (R_a) of the MEC using an on-line minimal resistance tracking (MRT) algorithm similar to

Table 1 – The operating conditions of acetate-fed MEC-A and sWW-fed MEC-W.

Phase description	MEC-A				MEC-W			
	Influent (g L^{-1})	HRT (h)	OLR (g L_R^{-1} d^{-1})	conductivity (mS cm^{-1})	Influent (g L^{-1})	HRT (h)	OLR (g L_R^{-1} d^{-1})	conductivity (mS cm^{-1})
(1) Standard	1.6	9.5	4.0	14.9	4.9	16.5	6.4	11.3
(2) Increased OLR	3.3	9.5	8.0	15.5	9.1	16.5	12.8	10.2
(3) HRT change	3.1	16.5	4.0	20.0	2.5	9.5	6.4	7.6
(4) Conductivity change	1.6	9.5	4.0	9.4	2.5	9.5	6.4	4.3

the perturbation and observation (P/O) method previously used to maximize power output of a microbial fuel cell [15]. A constant amplitude for each change of the applied voltage (ΔU) was preset and the direction of voltage change depended on the sign of the gradient determined using the finite difference method where the value of the internal resistance estimated at time t_i was compared with that estimated at the previous time instance t_{i-1}. This algorithm can be expressed by the following equation:

$$U(i) = U(i-1) + \Delta U \,\mathrm{sign}\left(\frac{R_{int}(i-1) - R_{int}(i-2)}{U(i-1) - U(i-2)}\right) \quad (1)$$

where ΔU is the input perturbation and i is the iteration number. In order to avoid MEC operation either at an applied voltage below the threshold value at which H_2 production can be observed or at an applied voltage corresponding to water electrolysis, the applied voltage is restricted:

$$U_{min} \le U(i) \le U_{max} \quad (2)$$

where U_{min} and U_{max} are the preset minimal and maximal allowable applied voltages. In all tests described below the minimal and maximal applied voltages were set to 0.3 V and 1.2 V, respectively.

As pointed out in Woodward et al. [15], with $i \to \infty$ the applied voltage will oscillate around the average (equilibrium) value U_{eq} with an amplitude of ΔU:

$$U(i) = \begin{cases} U_{eq} + \Delta U \\ \text{or} \\ U_{eq} - \Delta U \end{cases} \quad (3)$$

Since ΔU is the minimum step at which the applied voltage is changed, the maximum distance between the average of the oscillation (U_{eq}) and the true optimum value of the applied voltage (U^*) is $\Delta U/2$. A larger value of ΔU can be used to increase the speed of convergence if the algorithm starts far from the optimal point, but this choice of ΔU will result in a larger error in estimating optimal applied voltage when the applied voltage oscillates around U^*. A compromise between the convergence rate and the algorithm accuracy might be required.

3. Results and discussion

In theory, an U_{app} of only 0.14 V is required for microbially catalyzed electrolysis of acetate in a MEC [3]. Energy losses due to electrode overpotentials and solution resistance increase the voltage at which the onset of H_2 production is experimentally observed to 0.3–0.4 V [2,4]. Since the H_2 production rate is directly proportional to the current (I_{MEC}) and therefore increases at higher values of U_{app}, MECs are often operated at 0.8–1.0 V [6–8,16–19]. Importantly, the upper boundary of the U_{app} suitable for MEC operation is limited by the onset of water electrolysis, which theoretically requires an applied voltage of at least 1.2 V. Once again, electrode overpotentials and other energy losses bring this boundary closer to 1.8 V [2].

The exact choice of U_{app} might depend on the compromise between the desired rate of H_2 production and an acceptable rate of energy consumption. Indeed, MEC operation at higher U_{app} values results in increased production of H_2 but also in increased consumption of energy, since $P = U_{app} \cdot I_{MEC}$. The selection problem for the U_{app} can be illustrated by analyzing voltage scans.Fig. 1 shows typical voltage scans obtained in MECs fed with acetate and sWW. Prior to the voltage scans both MECs were operated at $U_{app} = 1$ V. Analysis of the graphs shows that regardless the type of carbon source the current and therefore H_2 production increases with increasing U_{app} until reaching a plateau. At the same time, power consumption, also plotted in Fig. 1, continues to increase with increasing U_{app}. If the rate of H_2 production should be maximized while avoiding excessive energy consumption, then U_{app} at which current first approaches the plateau might be the optimal value. The corresponding multi-criteria optimization problem can be formulated as:

$$\max_{U_{app}} J = \begin{bmatrix} F_{H_2} \\ -P \end{bmatrix} \quad (4)$$

where F_{H_2} is the H_2 flow rate and P is power consumption, $P = U_{app} \cdot I$.

Analysis of voltage scans shown in Fig. 1 suggests that the two requirements can be satisfied by operating a MEC at the inflection point of the power consumption curves. Furthermore, by plotting the apparent resistance (R_a) calculated as $R_a = U_{app}/I_{MEC}$ (dotted lines with circles in Fig. 1), we noticed that this inflection point corresponds to the minimal apparent resistance. This dependence could be proven using a MEC process model, such as the one presented by Pinto et al. [20]. Therefore, the multi-criteria optimization problem (4) can be

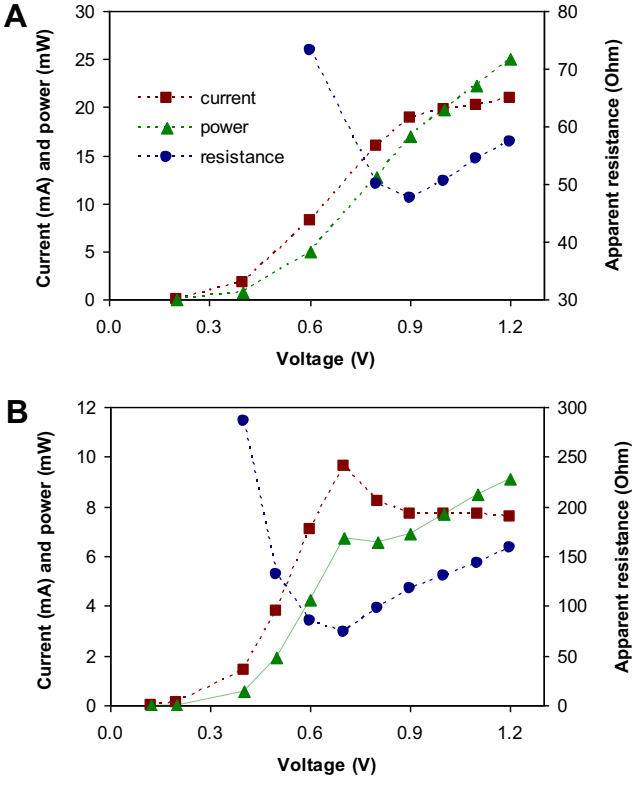

Fig. 1 – Voltage scans performed before the startup of real-time voltage control in MEC-A operated on acetate (A) and MEC-W operated on sWW (B). Apparent resistance was calculated as $R_a = U_{app}/I_{MEC}$.

reduced to a simpler problem of apparent resistance minimization:

$$\min_{U_{app}} R_a \quad (5)$$

As can be seen from the comparison of Fig. 1A and B, which were obtained during MEC-A and MEC-W operation on acetate and sWW, respectively, the value of U_{app} at which R_a approaches its minimum depends on the type of carbon source, but it might also depend on a number of other factors, such as influent concentration and composition, operating temperature, pH, solution conductivity and microbial populations. Therefore, a real-time algorithm for R_a minimization is required to track R_a variations over time. The minimal resistance tracking (MRT) method described in Materials and Methods was developed using the perturbation and observation (P/O) algorithm.

The proposed approach for maximizing H_2 production based on R_a minimization was tested in two MECs operated at different HRTs and different influent concentrations of the carbon source (either acetate or sWW). As mentioned above, both MECs were started at an U_{app} of 1.0 V and were operated at this voltage until observing stable H_2 production. Then the MRT algorithm was activated to control U_{app}. The startup of real-time U_{app} control during the MEC-A test resulted in a slight adjustment of U_{app}, as the algorithm immediately converged to $U_{app} = 1.09 \pm 0.05$ V (Fig. 2A). This suggested that the initial, expertise – based, choice of U_{app} was quite reasonable, at least for acetate as a source of carbon and the organic load used during phase 1 of the experiment. H_2 production rate stabilized at 2.8 ± 0.3 L/L$_R$/day with a corresponding acetate removal rate of 3.4 g/L$_R$/day. More details on process performance at a steady state are provided in Table 2.

To test the MRT algorithm robustness, several perturbations of operating conditions were imposed during MEC-A operation, including variations of acetate influent concentration and HRT as indicated in Table 1. An increase of influent acetate concentration from 1600 mg L^{-1} to 3300 mg L^{-1} had the most impact on optimal U_{app} and H_2 production. When acetate concentration in the influent was increased, U_{app} was almost immediately increased by the MRT algorithm and reached its upper limit set at 1.2 V (Fig. 3A). Accordingly, the MEC-A current increased to 30 mA and H_2 production reached 4.0 ± 0.2 L/L$_R$/day. Once the influent acetate concentration was returned to its previous value, the MRT algorithm promptly decreased the U_{app} returning MEC-A performance to its previous values (Fig. 3A and Table 1). At the same time, a change of HRT from 9.5 h to 16 h had no significant impact on MEC-A performance as can be seen from the results shown in Fig. 4A, which shows the transition period. In addition to the influent acetate concentration and HRT, the effect of solution conductivity on MEC-A performance was tested by

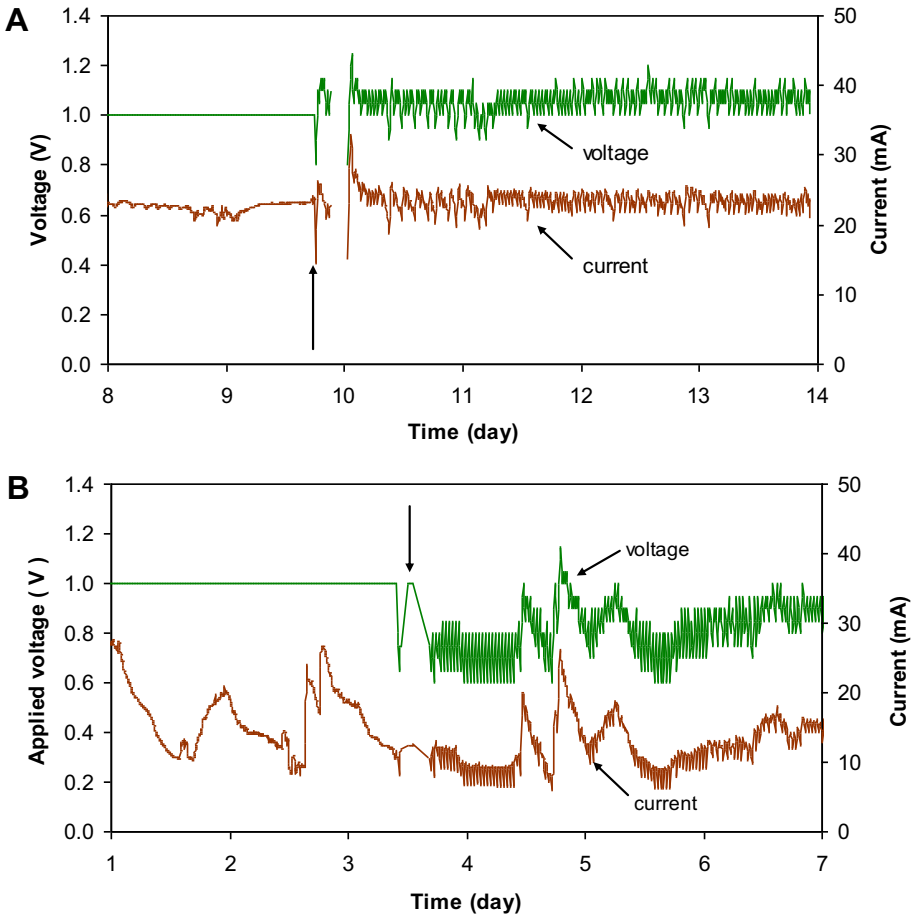

Fig. 2 – Current and voltage measurements in MEC-A (A) and MEC-W (B) before and after the startup of U_{app} optimization. The startup of real-time U_{app} control is indicated by arrows.

Table 2 – The performance of acetate-fed MEC-A.

Phase	U_{app}(V)	I_{MEC}(mA)	gas flow (L L_R^{-1} d^{-1})	H_2(%)	CH_4(%)	COD removal (g L_R^{-1} d^{-1})	Coulombic efficiency (%)
1	1.09 ± 0.05	23.3 ± 1.07	3.6 ± 0.4	79	3	3.4	79.1
2	1.2 ± 0.02	30.2 ± 0.76	4.6 ± 0.2	86	8	7.4	69.8
3	1.10 ± 0.04	24.7 ± 0.9	3.7 ± 0.3	79	13	4.2	81.5
4	1.10 ± 0.04	18.1 ± 0.9	3.4 ± 0.2	72	20	3.7	71.5

reducing concentration of the phosphate buffer, which reduced the conductivity of the effluent stream from 15 to 9 mS cm^{-1}. This had only minor impact on MEC performance as can be seen from the results presented in Table 1.

The MRT algorithm was also tested in MEC-W fed with sWW. As might be expected for a MEC operated on a complex carbon source requiring hydrolysis, at MEC-W startup both current and H_2 production were lower than in MEC-A at a comparable organic load (Table 2). Once the MRT algorithm was activated, U_{app} immediately decreased to 0.87 ± 0.06 V (Fig. 2B). This adjustment of U_{app} did not change the average current, which remained at 13.8 ± 1.9 mA. Also, the average H_2 production was unchanged. This signified the advantage of real-time control of U_{app}, which decreased power consumption without affecting process performance.

Notably, we observed significant fluctuations of U_{app} and, accordingly, I_{MEC} throughout the MEC-W test (Fig. 2B), which was different from the trends observed in MEC-A. These fluctuations were attributed to the changes in sWW stock solution composition over time. Significant fermentation of sWW in the syringe was observed through changes in the stock solution color and gas accumulation in the syringe. This was confirmed through VFA and COD analysis. While total COD content of the stock solution remained unchanged, acetate and propionate concentrations of the stock solution were measured to increase from near zero values to over 1000 mg L^{-1} after 4 days in the syringe indicating ongoing hydrolysis and fermentation of the proteins. This change in influent composition was reflected in decreased MEC performance immediately after each replacement of the syringe, when VFA concentration was low, followed by a progressive increase of current corresponding to increased VFA concentration (Fig. 2B). This behavior suggested that the hydrolysis and fermentation of proteins in the fresh sWW stock solution

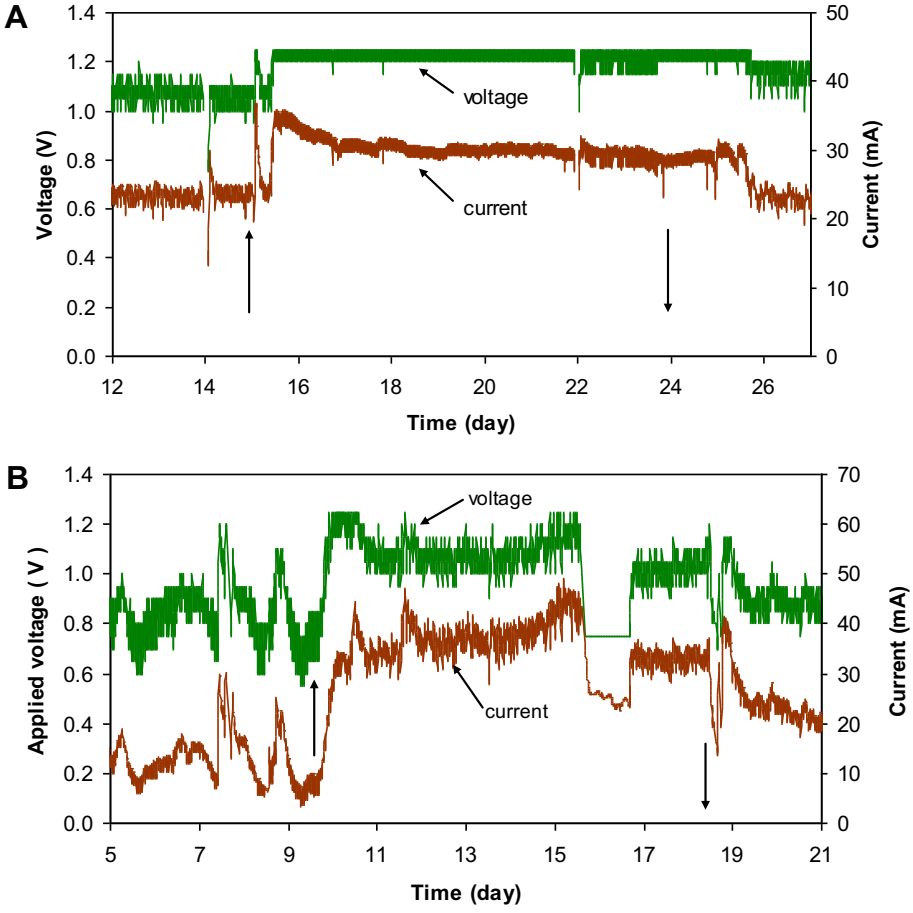

Fig. 3 – MEC performance response to an increase and decrease of influent concentration of (A) acetate in MEC-A and (B) sWW in MEC-W. The U_{app} was controlled by the MRT algorithm. The influent concentration changes are indicated by arrows.

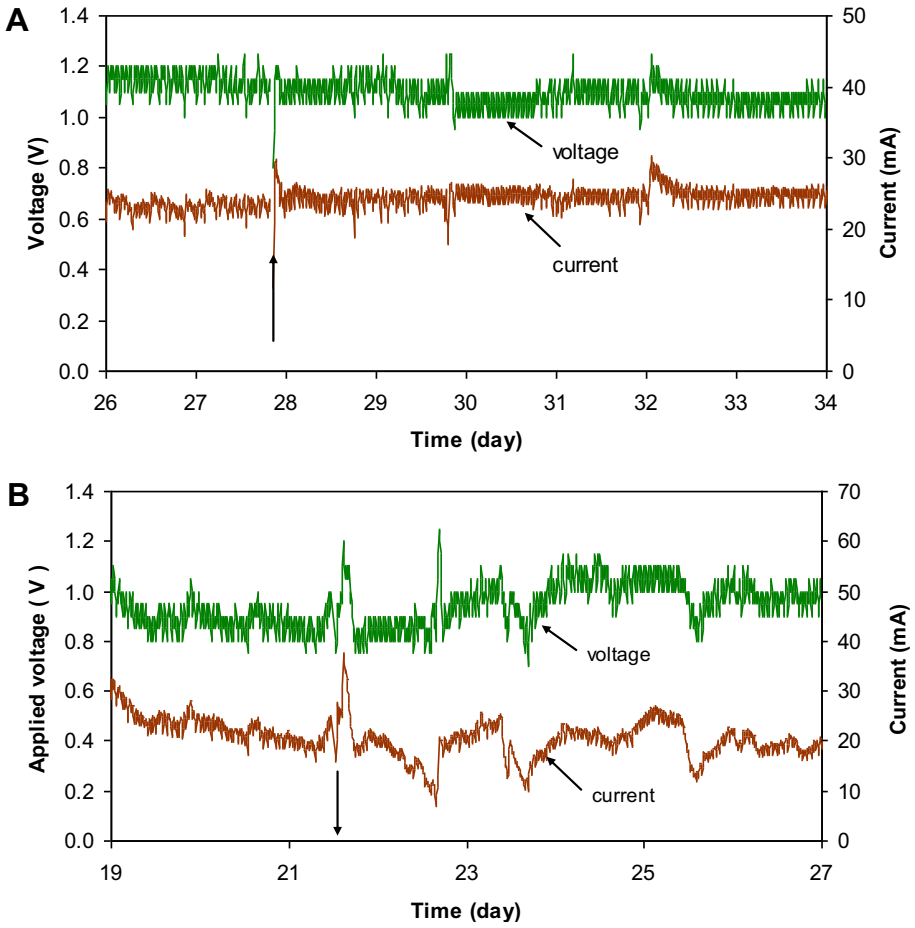

Fig. 4 – MEC performance response to HRT changes during (A) MEC-A operation when HRT was increased from 8.5 h to 17 h and (B) MEC-W operation when HRT was decreased from 17 h to 8.5 h. HRT changes are indicated by arrows.

limited the rate of carbon source consumption by the exoelectricigenic microorganisms. Nevertheless, the MRT algorithm was capable of accurately tracking the variations in the carbon source properties by adjusting U_{app}. The varying composition of the stock solution due to protein hydrolysis and fermentation might resemble variations in wastewater composition during MEC operation on real wastewater. Therefore the sWW tests with a varying stock composition confirmed the excellent tracking performance of the algorithm and its applicability for large scale MEC operation.

As in the previous test with acetate, MEC-W was subjected to several external perturbations, including changes in the influent concentration (i.e. sWW strength) and HRT. Fig. 3B shows the response of the MRT algorithm to increased COD concentration in the influent. The response was significant and similar to that observed in MEC-A. Once fresh sWW media was added to the syringe, MEC performance at first declined, but then rebounded as the media fermented, with U_{app} and current approaching 1 V and 35 mA, respectively (Fig. 3B) and accordingly, H_2 production increased to 5.3 ± 0.8 L L_R^{-1} d^{-1}. While MEC operation at a high organic load resulted in increased H_2 production, the COD removal efficiency was relatively low at 68%, although the COD removal rate was at 8.7 g L_R^{-1} d^{-1}. This was indicative of organic overload. More details are shown in Table 3.

MEC-W response to HRT changes was also similar to the trends observed in MEC-A test. MEC-W operation was started at an HRT of 17 h, which was greater than that of MEC-A, with an HRT of 9.5 h. It was hypothesized that more time might be required for protein hydrolysis when feeding sWW. On day 21.5 HRT was decreased to 8.5 h. No significant response to this perturbation was observed, with current variations due to syringe replacement having a more significant impact than the change of HRT, as can be seen from Fig. 4B.

In addition to the tests described above, robustness of the MRT algorithm was also shown in the accidental feed interruptions caused by syringe pump malfunctions or late replacement of the syringe with the stock solution. In both MEC-A and MEC-W such an event was followed by decreased U_{app} and current as the carbon source in the anodic compartment became exhausted. The algorithm, however, returned the U_{app} to its previous value once the feeding was resumed (Fig. 5). Another interesting feature of the MRT algorithm was that it appeared to reduce the presence of methane in the cathodic gas stream. The presence of hydrogenotrophic methanogens in MECs results in H_2 conversion to methane. The amount of H_2 lost to methane production appears to increase if a MEC is operated at low values of U_{app} [4,21,22]. In extreme cases more than 20% of the cathodic gas stream is composed of methane in particular when operating

Table 3 – The performance of sWW-fed MEC-W.

Phase	U_{app}(V)	I_{MEC} (mA)	gas flow (L L_R^{-1} d^{-1})	H_2 (%)	CH_4(%)	COD removal g L_R^{-1} d^{-1}	Coulombic efficiency (%)
1	0.88 ± 0.05	22.2 ± 2.2	2.3 ± 0.8	91	3	5.1	53.9
2	1.02 ± 0.05	33.2 ± 1.7	5.3 ± 0.8	92	2	8.7	52.5
3	0.98 ± 0.04	20 ± 1.4	2.3 ± 0.4	92	3	5.0	59.5
4	0.99 ± 0.06	20.2 ± 3.2	2.6 ± 0.8	73	3	4.7	56.4

on wastewater [4,5]. In our tests, MEC-W was continuously operated for 45 days. Although the methane percentage appeared to be dependent on organic load with less methane observed at the highest influent COD concentration, only 2–10% of methane were observed in the cathodic gas stream (Table 3), while methane production in the anodic compartment was negligible.

Voltage scans, which were performed at the end of each phase of operation, also confirmed the MRT algorithm reliability. After each test minimal apparent resistance was estimated from R_a vs U_{app} graphs as shown in Fig. 1 and the corresponding value of optimal applied voltage was determined. Fig. 6 shows a comparison of the optimal applied voltages (U_{opt}) estimated for both MECs based on the results of the voltage scans with the average U_{opt} values estimated by the MRT algorithm during the 2 h preceding each voltage scan. Good statistical agreement was obtained with R^2 equal to 0.85.

The MEC tests were conducted with a potentiostat to maintain a constant anode potential vs. a reference electrode. The results showed the fastest biofilm growth and the highest current density when the anodes were maintained at the lowest potentials [23]. This is in agreement with the voltage scans shown in Fig. 1, where the current reaches a plateau at higher applied voltages corresponding to more negative anode potentials. Importantly, the MRT algorithm presented in this work did not require a reference electrode. For practical purposes of wastewater treatment the anode potential measurements against a reference electrode placed in the anodic compartment would be troublesome due to biofilm growth at the electrode surface. The MRT algorithm, which only uses the two electrode (anode–cathode) setup, could be

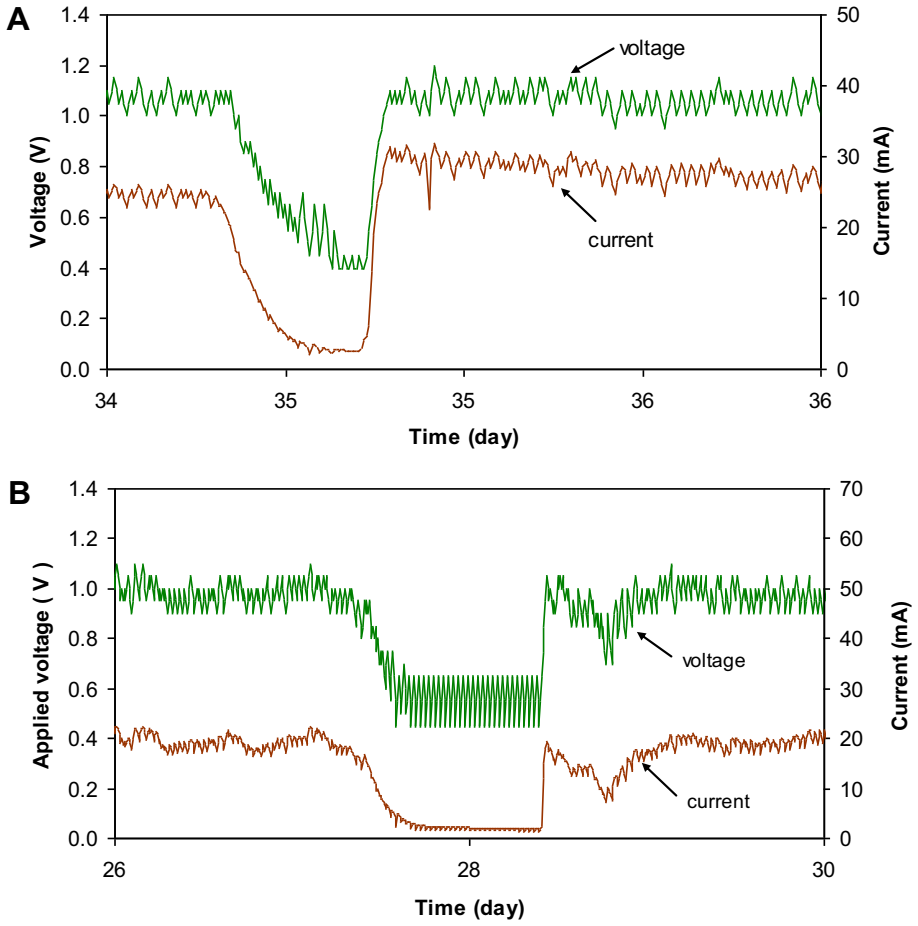

Fig. 5 – Examples of MRT algorithm response to feed interruptions in (A) MEC-A fed with acetate and in (B) MEC-W fed with sWW.

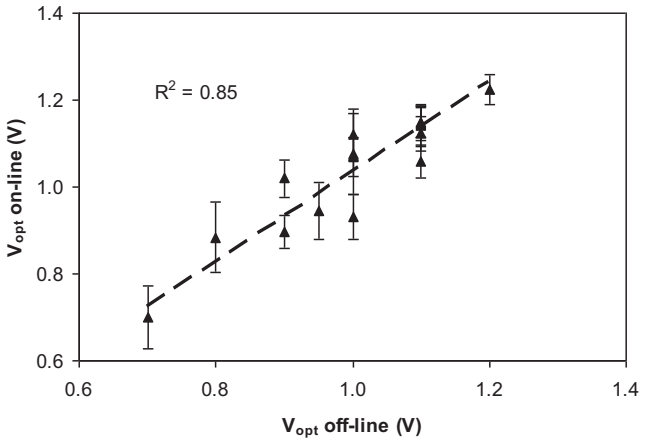

Fig. 6 – A comparison of optimal values of U_{app} estimated from the results of voltage scans in MEC-A and MEC-W with the average U_{app} values maintained by the MRT algorithm during 2 h preceding each voltage scan.

used in a variety of MEC configurations, sizes, and with various types of wastewater.

4. Conclusion

This work demonstrates the advantages of real-time control of U_{app} for maximizing H_2 production in a MEC. It is shown that MEC performance can be optimized by minimizing the apparent resistance ($R_a = U_{app}/I_{MEC}$). Furthermore, a minimal resistance tracking algorithm was proposed and tested in laboratory-scale MECs. The tests performed using acetate or sWW as a source of carbon confirmed the excellent robustness of the proposed algorithm. The real-time control of U_{app} demonstrated in this work might be an essential component in the development of industrial MEC-based technologies for simultaneous H_2 production and wastewater treatment.

Acknowledgment

This is NRC manuscript no 53364.

REFERENCES

[1] Logan BE, Call D, Cheng S, Hamelers HVM, Sleutels THJA, Jeremiasse AW, et al. Microbial electrolysis cells for high yield hydrogen gas production from organic matter. Env Sci Technol 2008;42:8630–40.
[2] Liu H, Grot S, Logan BE. Electrochemically assisted microbial production of hydrogen from acetate. Env Sci Technol 2005; 39:4317–20.
[3] Rozendal RA, Hamelers HVM, Euverink GJW, Metz SJ, Buisman CJN. Principle and perspectives of hydrogen production through biocatalyzed electrolysis. Int J Hydrogen Energ 2006;31:1632–40.
[4] Ditzig J, Liu H, Logan BE. Production of hydrogen from domestic wastewater using a bioelectrochemically assisted microbial reactor (BEAMR). Int J Hydrogen Energ 2007;32: 2296–304.
[5] Wagner RC, Regan JM, Oh SE, Zuo Y, Logan BE. Hydrogen and methane production from swine wastewater using microbial electrolysis cells. Wat Res 2009;43:1480–8.
[6] Hrapovic S, Manuel MF, Luong JHT, Guiot SR, Tartakovsky B. Electrodeposition of nickel particles on a gas diffusion cathode for hydrogen production in a microbial electrolysis cell. Int J Hydrogen Energ 2010;35:7313–20.
[7] Tartakovsky B, Manuel MF, Wang H, Guiot SR. High rate membrane-less microbial electrolysis cell for continuous hydrogen production. Int J Hydrogen Energ 2009;34:672–7.
[8] Hu H, Fan Y, Liu H. Hydrogen production in single-chamber tubular microbial electrolysis cells using non-precious-metal catalysts. Int J Hydrogen Energy 2009;34:8535–42.
[9] Selembo PA, Merill MD, Logan BE. The use of stainless steel and nickel alloys as low-cost cathodes in microbial electrolysis cells. J Power Sources 2009;109:271–8.
[10] Harnisch F, Sievers G, Schroder U. Tungsten carbide as electrocatalyst for the hydrogen evolution reaction in pH neutral electrolyte solutions. Appl Catal B Environ 2009;89: 455–8.
[11] Zhong Z, Huo H, Zhu X, Cao G, Ren Y. Adaptive maximum power point tracking control of fuel cell power plants. J Power Sources 2008;176:259–69.
[12] Manuel M-F, Neburchilov V, Wang H, Guiot SR, Tartakovsky B. Hydrogen production in a microbial electrolysis cell with nickel-based gas diffusion cathodes. J Power Sources; 2010:195.
[13] Tartakovsky B, Manuel MF, Neburchilov V, Wang H, Guiot SR. Biocatalyzed hydrogen production in a continuous flow microbial fuel cell with a gas phase cathode. J Power Sources 2008;182:291–7.
[14] Escapa A, Manuel M-F, Morán A, Gómez X, Guiot SR, Tartakovsky B. Hydrogen production from glycerol in a membrane-less microbial electrolysis cell. Energy and Fuels 2009;23:4612–8.
[15] Woodward L, Perrier M, Srinivasan B, Pinto RP, Tartakovsky B. Comparison of real-time methods for maximizing power output in microbial fuel cells. AIChE J 2010;56:2742–50.
[16] Chae KJ, Choi MJ, Lee J, Ajayi FF, Kim IS. Biohydrogen production via biocatalyzed electrolysis in acetate-fed bioelectrochemical cells and microbial community analysis. Int J Hydrogen Energ 2008;33:5184–92.
[17] Lee H-S, Torres CI, Parameswaran P, Rittmann BE. Fate of H2 in an upflow single-chamber microbial electrolysis cell using a metal-catalyst-free cathode. Env Sci Technol 2009;43:7971–6.
[18] Rozendal RA, Jeremiasse AW, Hamelers HVM, Buisman CJN. Hydrogen production with a microbial biocathode. Environ Sci Technol 2008;42:629–34.
[19] Selembo PA, Merrill MD, Logan BE. Hydrogen production with nickel powder cathode catalysts in microbial electrolysis cells. Int J Hydrogen Energ 2010;35:428–37.
[20] Pinto RP, Srinivasan B, Escapa A, Tartakovsky B. Multi-Population model of a microbial electrolysis cell. Env Sci Technol 2011;45:5039–46.
[21] Clauwaert P, Verstraete W. Methanogenesis in membraneless microbial electrolysis cells. Appl Microbiol Biotechnol 2008;82:829–36.
[22] Sleutels THJA, Lodder R, Hamelers HVM, Buisman CJN. Improved performance of porous bio-anodes in microbial electrolysis cells by enhancing mass and charge transport. Int J Hydrogen Energ 2009;34:9655–61.
[23] Torres CI, Krajmalnik-Brown R, Parameswaran P, Marcus AK, Wanger G, Gorby YA, et al. Selecting anode-respiring bacteria based on anode potential: phylogenetic, electrochemical, and microscopic characterization. Eviron Sci Technol 2009; 43:9519–24.